Penerbit Akademia Baru

Journal of Advanced Research in Materials Science
ISSN (online): 2289-7992 | Vol. 11, No.1. Pages 8-19, 2015

Enhancing Interfacial Adhesion of Potash Feldspar with Silane (Si-69) Coupling Agent on Properties of Ethylene Vinyl Acetate (EVA)/ Natural Rubber (NR)/ Potash Feldspar Composites

S. H. Ho [*,1,a], *A. G. Supri*[2,b], *and H. Ismail*[3]

[1]Faculty of Engineering Technology, Universiti Malaysia Perlis (UniMAP), Main Campus, Pauh Putra, Perlis, Malaysia.
[2]School of Materials Engineering, Universiti Malaysia Perlis (UniMAP), Kompleks Taman Muhibah, Jejawi 2, 02600, Perlis, Malaysia.
[3]School of Materials and Mineral Resources Engineering, Universiti Sains Malaysia, Nibong Tebal, Penang, 14300 Malaysia.
[a,*]*hoshuhhuey_1989@yahoo.com,* [b]*supri@unimap.edu.my*

Abstract – *The untreated and treated ethylene vinyl acetate/ natural rubber/ potash feldspar (EVA/NR/PF) composites were prepared using Brabender Plasticoder at 160°C and rotor speed of 50 rpm. The tensile strength and modulus at 100% elongation for EVA/NR/PF$_{Silane}$ composites increased while the elongation at break and mass swell were decreased as the PF loading increased. EVA/NR/PF$_{Silane}$ composites exhibited lower degree of crystallinity but higher thermal stability in comparison to EVA/NR/PF composites. The SEM morphology for EVA/NR/PF$_{Silane}$ composites exhibited rough surface which improved the interfacial adhesion between filer and polymer matrix.*

Keywords: Potash Feldspar, ethylene vinyl acetate, natural rubber, silane coupling agent

1.0 INTRODUCTION

Thermoplastic elastomers (TPEs) are elastomers that can be processed like a thermoplastic. TPEs have the physical properties of conventional elastomers at room and service temperatures, and excellent processing characteristics of thermoplastic materials at high temperature. TPEs have economic advantages, good processability and reprocessable [1]. The continuous plastic matrix allow the melt processing of the blend and the dispersed rubber phase provide the elasticity of the blend after deformation. Most of the thermoplastic and rubber blend are incompatible [2]. Due to the weak bond between the soft phase from the elastomer and the hard phase from the thermoplastics, the thermoplastic elastomer perform poor tensile properties. Coupling agents or compatibilizers are the third components added to the polymer mixture in order to improve the coupling of the two phases [3].

Particulate fillers reinforced the polymer matrix and modified the mechanical performance of the particulate composites. The mechanical properties of particle-filled composites are

influenced by the filler concentration, filler size and shape, and the interfacial strength of the filler [4]. Particulate filler modified with coupling agents are often used to reduce the agglomeration in polymer composites [5]. Surface treatments for particulate fillers is necessary due to many of the polymer are non-polar and hydrophobic while particulate are highly hydrophilic [6].

Less compatibility between the polymers and worst dispersion can be caused by the large differences in surface tensions between the polymer and fillers. Therefore, surface treatment of the fillers can be performed to improve the compatibility, and the quality and stability of filler dispersion in polymer matrices [7]. By the surface modifications using silane coupling agents into the composites, the matrix-filler interaction which formed by one end of molecule is attached to the reinforcement surface while the other end reacts with the polymer phase is improved. Coupling agents is chemical that improved the interfacial adhesion by create chemical bridge between the reinforcement and the matrix at the interface when one end of the molecule attached to the surface of the reinforcement and the other end reacts with the polymer phase [8]. The interfacial compatibilization lowers the interfacial tension, improve the adhesion between the phases, stabilizes the microstructure and decrease the dispersed phase domain size [9].

This paper reports the effect of treated potash feldspar with silane coupling agent on tensile properties, morphology, thermal properties, swelling behavior, and thermal degradation of ethylene vinyl acetate/ natural rubber/ potash feldspar composites.

2.0 EXPERIMENTAL

Materials

Ethylene vinyl acetate (EVA) contains 18.1 wt% VA was obtained from The Polyolefin Company (Singapore) Pte.Ltd. Natural rubber (SMR-L) was purchased from Rubber Research Institute of Malaysia (RRIM). Potash Feldspar (PF) with the average particle size of 10.2 µm was obtained from Commercial Minerals (M) Sdn. Bhd., Penang, Malaysia. Ethanol 98% (C_2H_5OH) and Silane (Si-69) were obtained from A.R. Alatan Sdn Bhd, Alor Setar, Kedah, Malaysia. The chemical composition and physical properties of potash feldspar are given in Table 1.

Filler Treatment

The Potash Feldspar was treated with silane coupling agent (S-i69). 3 wt % of silane coupling agent was added into the 100ml of ethanol and was stirred using the magnetic stirrer for 1 hour. After that, 100 grams of potash feldspar was transferred into the solution and was stirred for another 1 hour. The mixtures was then dried in oven at 100ºC for 24 hours.

Composite Preparation

The compounding was carried out by melt blending using Brabender Plasticoder at the temperature of 160˚C and rotor speed of 50 rpm. The EVA was loaded into the mixing chamber for 3 minutes until it melted. After that, natural rubber (NR) was added into the mixing chamber until the mixture was homogenous. Then, the treated or untreated potash feldspar was incorporated into the mixture for 3 minutes. The total mixing time was 10 minutes. The soften blend was removed from the chamber and pressed into thick round pieces. The formulations of of EVA/NR/PF composites and EVA/NR/PF_{Silane} composites are shown in Table 2.

Table 1: Chemical and physical properties of potash feldspar

Chemical Composition	Value (%)
SiO	67.0
Al_2O_3	19.0
CaO	0.11
Na_2O	2.3
P_2O_5	0.18
SO_3	0.028
K_2O	11.0
Fe_2O_3	0.12
NiO	0.025
Rb_2O	0.28
Ignition loss	0.2
Physical Properties	
Mean particle size (µm)	10.18
Surface area (m^2/g)	0.73
Density (g/m^3)	2.0

Table 2: Formulation of the EVA/NR blend with silane treated PF

EVA/NR (phr)	*PF (phr)
70/30	0
	5
	10
	15
	20
	25

*PF modified with silane coupling agent

Compression Moulding

Compounds were moulded into 1 mm thin sheet using the hydraulic hot press. The temperature was set at 160˚C for both the top and bottom platen. The empty mould was heated for 4 minutes. The composites were preheated for 4 minutes. Once the composites started to soften they were fully compressed for 4 minutes. After compression, the composites were allowed to cool for 3 minutes.

Tensile Test

EVA/NR/PF composites and EVA/NR/PF_{Silane} composites sheets were cut into dumbbell shaped using the dumbbell cutter. Tensile tests were carried out according to ASTM D421 by using Instron 5569 with crosshead speed of 50 mm/min. The tensile strength, elongation at break and modulus at 100% elongation (M100) were obtained from the test for each composition.

Swelling Behavior Test

Mass swell test was carried out by immersed three samples of each composites with the dimension of 20mm x 10mm x 10mm into toluene for 46 hours at room temperature according to ISO 1817. The samples were weighed before the immersion. After the immersion period, the samples were wiped with tissue and weighed by using an analytical balanced with 0.1mg resolution. The mass swell percentage (% MS) was calculated using equation 1.

$$\% MS = \frac{W_2 - W_1}{W_1} x\ 100\% \quad (1)$$

Where W_2 is the weight of wet sample and W_1 is the weight of dry sample.

Scanning Electron Microscopy (SEM) Analysis

The morphology of the fracture surfaces of composite were studied by using scanning electron microscope model JOEL JSM-6460LA. The samples were mounted on aluminium stubs and allowed to undergo sputtering coating before the examination of SEM. A thin gold layer of 20 nm was sputter coated on the samples surfaces to avoid electrostatic charged during examination.

Fourier Transform Infrared (FT-IR) Spectroscopy

The chemical groups for EVA/NR/PF composites and EVA/NR/PF_{Silane} composites were analysed using Perkin-Elmer Spectrum One Series equipment and the sample was prepared by grind 10mg of the sample with Potassium bromide (KBr). The selected spectrum resolution and the scanning range were 4 cm^{-1} and 600-4000 cm^{-1} respectively.

Differential Scanning Calorimetry

Thermal analysis measurements of selected system were performed using a Perkin Elmer DSC-7 analyzer. Samples of about 4 mg were heated from 25 to 250^0C using a nitrogen air flow of 50 ml/min and heating rate of 10^0C/min. The melting and crystallization behavior of selected sample also performed using a Perkin Elmer DSC-7 analyzer. The crystallinity of sample was determined using Eqn. 2.

$$Crytallinity = \frac{\Delta H_f}{\Delta H^0{}_f} \times 100\% \quad (2)$$

Where ΔH_f and ΔH^o_f are enthalpy of fusion of the composite and enthalpy of fusion of EVA, respectively. ΔH^o_f based on EVA containing 18wt% VA content are reported 68J/g [10].

Thermogravimetric Analysis

The thermal analysis was carried out by using TGA Diamond, Perkin-Elmer apparatus. Thermogravimetric analysis (TGA) involves heating a sample in an inert or oxidized atmosphere and measuring the weight. The weight change over specific temperature ranges provides indications of the composition of the sample and thermal stability. Thus, the thermal stability of sample can be studied through the onset temperature and decomposition temperature from the TGA result. The sample of about 10 mg in weight was placed into platinum crucible and was heated from 30ºC to 850ºC at heating rate of 10ºC/min under nitrogen atmosphere condition with the nitrogen flow rate of 50 ml/min. The temperature at 50% weight loss ($T_{-50\%wt}$), final decomposition temperature and residual mass were calculated.

3.0 RESULTS AND DISCUSSION

Figure 1 illustrates the effect of filler loading on tensile strength of EVA/NR/PF and EVA/NR/PF_{Silane} composites. The tensile strength for both composites decreased as the filler loading increased. An increased in the PF loading would increase the amount of filler to

Penerbit Akademia Baru

Journal of Advanced Research in Materials Science
ISSN (online): 2289-7992 | Vol. 11, No.1. Pages 8-19, 2015

aggregate and would not wetted by the matrix phases. Agglomeration of the PF at the interface will create the stress-concentration point which caused the composites to break when forces are applied into it. Besides, the fillers were unable to support the stress transfer from the polymer matrix.

By compared both composites, EVA/NR/PF_{Silane} composites show higher tensile strength than EVA/NR/PF composites. This was due to the reaction between the hydroxyl group of the silane coupling agents and the EVA and NR phases. Chemical bonding formed when silanol reacts with the hydroxyl group of the filler surface and the organic group will reacts with the matrix. This linkages at the filler matrix interface acts as a molecular bridge that allow the composites to transfer the stress from the matrix to the PF during loading, thereby the strength is improved. Similar observation by Alkadasi et al. [11], claimed that treatment of fly ash with coupling agent which is Bis (3-triethoxy-silyl propyl) tetrasulphide had enhanced the tensile strength, modulus at 100, and 400 elongation as the result of the improvement in the filler-matrix adhesion.

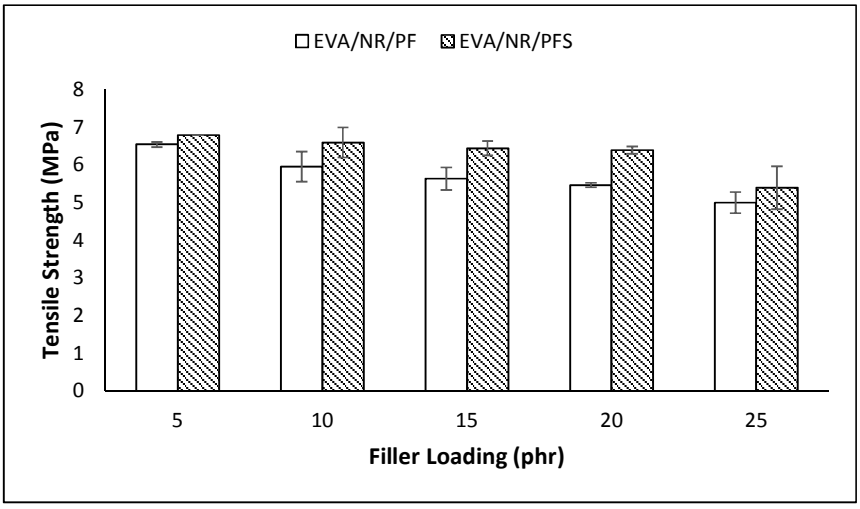

Figure 1: Tensile strength vs filler loading of EVA/NR/PF and EVA/NR/PF_{Silane} composites

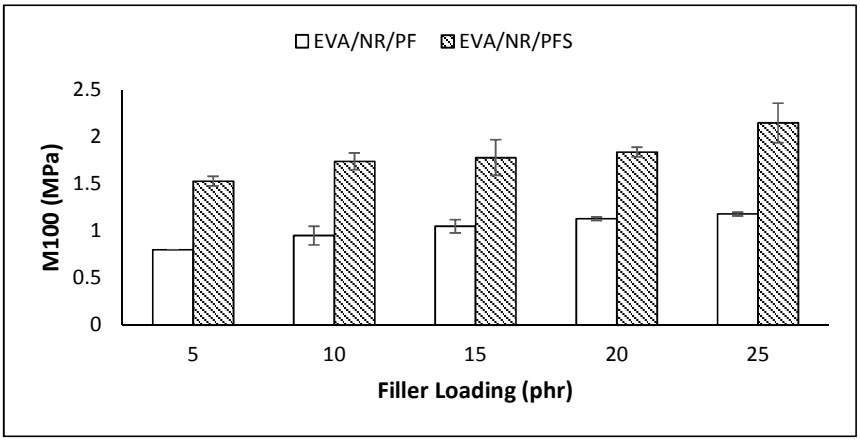

Figure 2: Modulus at 100% elongation (M100) vs filler loading of EVA/NR/PF and EVA/NR/PF_{Silane} composites

Journal of Advanced Research in Materials Science
ISSN (online): 2289-7992 | Vol. 11, No.1. Pages 8-19, 2015

Figure 2 shows modulus at 100% elongation (M100) of EVA/NR/PF and EVA/NR/PF_{Silane} composites. M100 of EVA/NR/PF and EVA/NR/PF_{Silane} composites increased as the filler loading increased. This resulted from the addition of the rigid filler particle into the matrix. Thereby, restriction of the mobility of polymer molecules increased the M100 of the composites.

Besides, EVA/NR/PF_{Silane} composites show higher M100 compared to EVA/NR/PF composites. This can be attributed to strong interface between the silane treated PF and matrix. Improvement in the filler-matrix adhesion had attributed to the stiffness of the composites. Ganguly et al. [12] reported that the modulus at 100% elongation for all modified compound have greater value.

Figure 3 illustrates the elongation at break of EVA/NR/PF and EVA/NR/PF_{Silane} composites. The elongation at break for EVA/NR/PF and EVA/NR/PF_{Silane} composites decreased as the PF loading increased. The addition of filler into the soft matrix reduced the flexibility and elasticity of the polymer chain, resulting a more rigid composites.

By comparing both composites, EVA/NR/PF_{Silane} composites had lower elongation at break. This can be explained by better stiffness achieved from the strong adhesion between the matrix and the filler. The improvement of the filler-matrix adhesion will caused lower extension. With the silane treated, effective wetting of the filler by polymer matrix occurred in EVA/NR/PF_{Silane} composites.

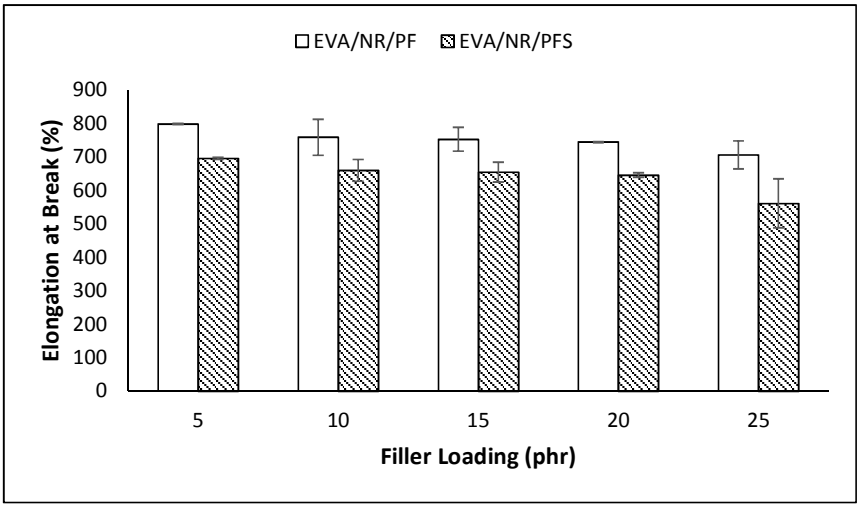

Figure 3: Elongation at break vs filler loading of EVA/NR/PF and EVA/NR/PF_{Silane} composites

Mass swell percentage of EVA/NR/PF and EVA/NR/PF_{Silane} composites are shown in Figure 4. From the Figure 4, mass swell percentage for both composites were decreased as the PF loading increased. As the PF loading increased, the interparticle spacing between the filler and the matrix decreased. The free volume for the toluene to penetrate into the composites were limited. Hence, the mass swell percentage for both composites decreased as the PF loading increased.

Penerbit Akademia Baru

Journal of Advanced Research in Materials Science
ISSN (online): 2289-7992 | Vol. 11, No.1. Pages 8-19, 2015

From the Figure 4, EVA/NR/PF_{Silane} composites has lower mass swell percentage in comparison with EVA/NR/PF composites. This can be explained by the crosslinking structure formed in the EVA/NR/PF_{Silane} composites in which the free spaces for toluene to penetrate into the composites are limited. Hence, less toluene can penetrate into the composites. Park et al. [13] obtained that the crosslink density for the silane treated composites is increased, hence the weight swelling for the silane treated silica/γ -aminopropyl triethoxysilane (APS), silica/γ -chloropropyl trimethoxysilane (CPS), and silica/γ - methacryloxypropyl trimethoxysilane (MPS) is lower than untreated ones.

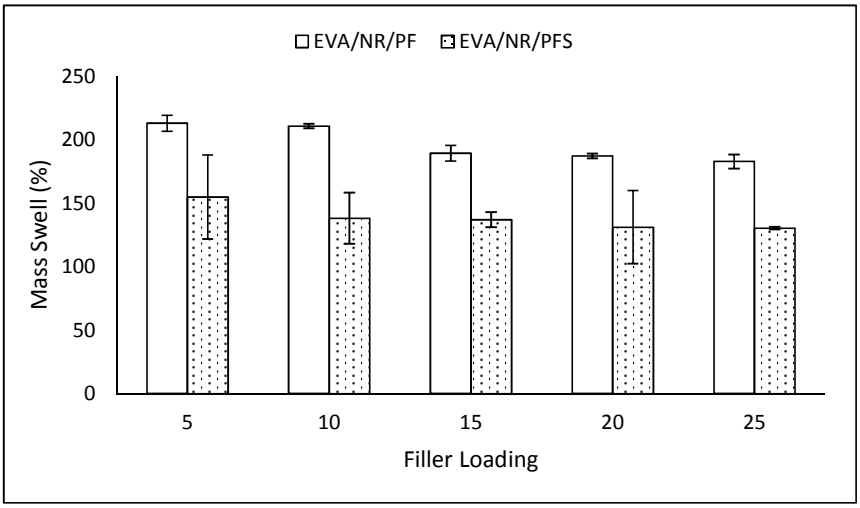

Figure 4: Mass swell percentage vs filler loading of EVA/NR/PF and EVA/NR/PF_{Silane} composites

The SEM micrograph of tensile fracture surfaces of the EVA/NR/PF and EVA/NR/PF_{Silane} composites with different of filler loading is shown in Figure 5. Figure 5 (a), (b), and (c) shows poor wettability and poor adhesion of the filler with the EVA/NR matrix. Detachment of the PF from the matrix is the main factors. With the silane treated PF, the micrograph shows better adhesion and interactions between the PF and the matrix phases. The well dispersion of the PF into the matrix resulted in higher tensile strength compared to EVA/NR/PF composites. This may be due to the ability of the silane to reduce the surface energy and the filler-filler interaction. Bigui et al. [14] reported the SEM images for silane modified quartz sand surface are flatter than unmodified due to the surface of the quartz sand filler has been grafted by the silane coupling agent.

Figure 6 illustrates FTIR spectrum of EVA/NR/PF_{Silane} composites with 15 phr of PF. The weak O-H bond had the characteristics absorption at 721.47 cm^{-1}. The peak at 1020.86 and 1099.6 cm^{-1} proved the presence of the strong C-O from EVA. CH_3 deformation and CH_3, CH_2 deformation show absorptions at peaks 1373.6 and 1456 cm^{-1}. The spectrum shows C-H strong saturated ester (C=O) at the peak of 1739 cm^{-1}. Strong CH_3, CH_2 and CH has the characteristic absorptions at 2918.57 and 2850.43 cm^{-1}.

Figure 7 shows the DSC thermograms of EVA/NR/PF_{Silane} composites and Table 3 shows the melting temperature (T_m) and percentage of crystallinity of EVA/NR/PF and EVA/NR/PF_{Silane} composites at different PF loading. From Table 3, it can be seen that the melting temperature of both composites increase slightly with the increasing potash feldspar loading. The melting

Penerbit Akademia Baru

Journal of Advanced Research in Materials Science
ISSN (online): 2289-7992 | Vol. 11, No.1. Pages 8-19, 2015

temperature (T_m) of EVA/NR/PF_{Silane} composites is slightly higher than EVA/NR/PF composites due to the better interfacial adhesion between EVA/NR phases and potash feldspar with the presence of silane (Si-69) coupling agent.

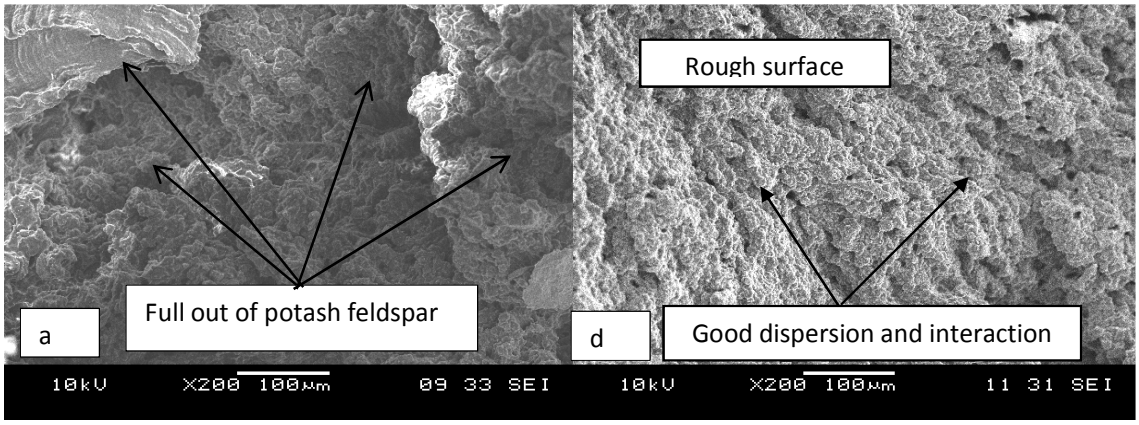

(a) EVA/NR/5PF (a) EVA/NR/5PF_{Silane}

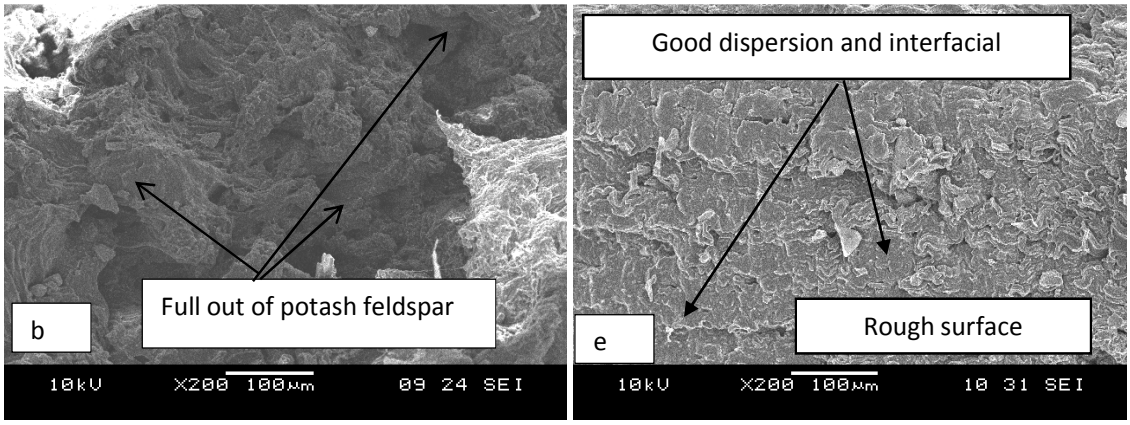

(b) EVA/NR/15PF (e) EVA/NR/15PF_{Silane}

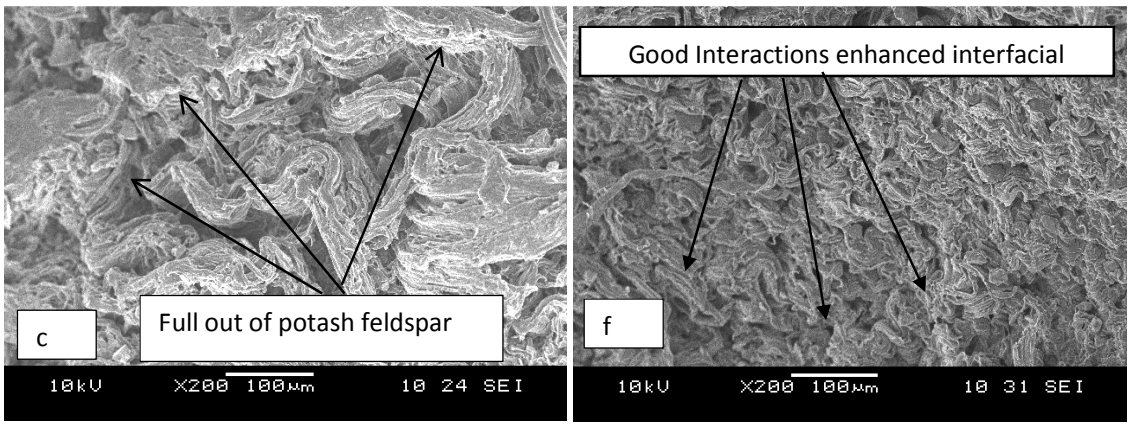

(c) EVA/NR/25PF (f) EVA/NR/25PF_{Silane}

Figure 5: SEM micrograph of tensile fracture surfaces of the EVA/NR/PF and EVA/NR/PF_{Silane} composites with different of filler loading

Penerbit Akademia Baru
Journal of Advanced Research in Materials Science
ISSN (online): 2289-7992 | Vol. 11, No.1. Pages 8-19, 2015

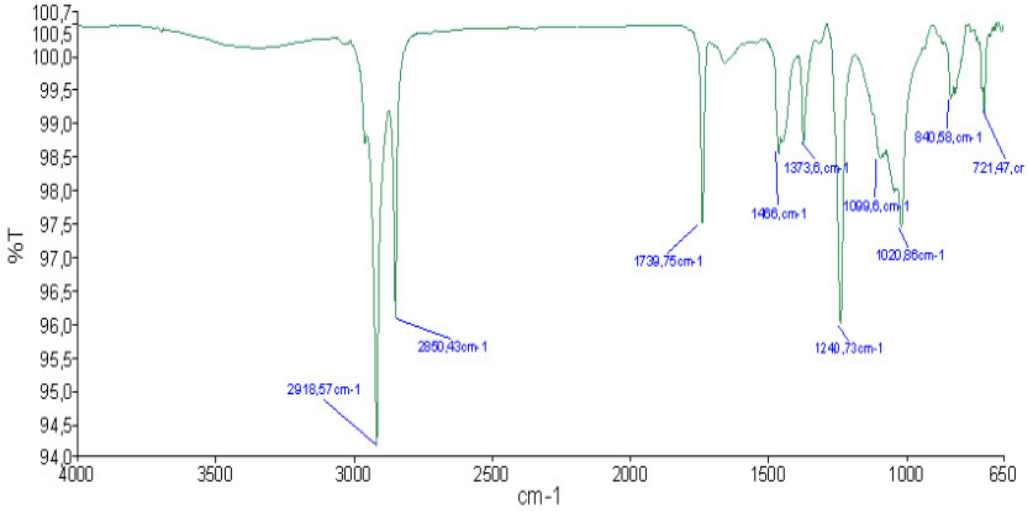

Figure 6: FTIR spectra of EVA/NR/PF$_{Silane}$ composites with 15phr of PF

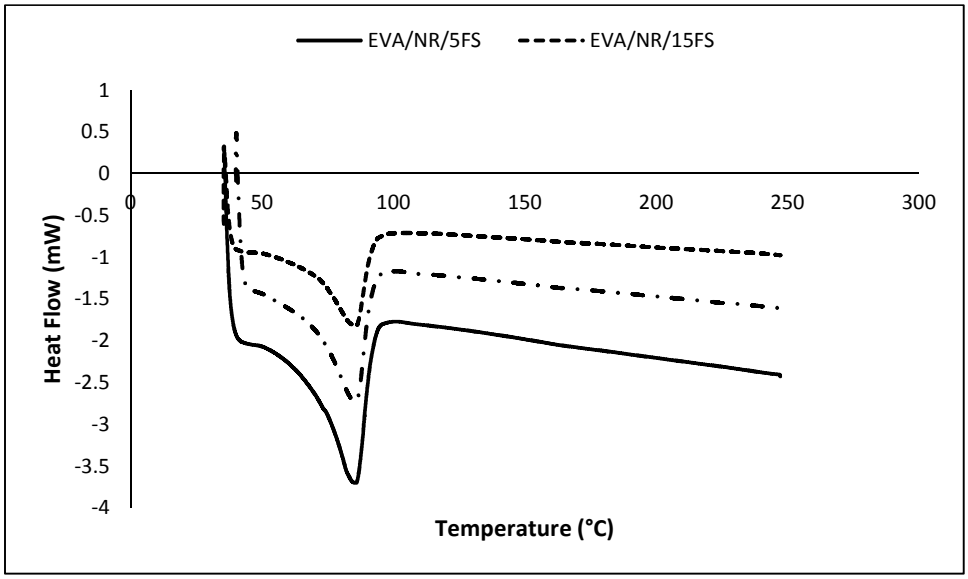

Figure 7: DSC thermograms of EVA/NR/PF$_{Silane}$ composites

The result also shows the percentage of crystallinity of both composites increased with increasing filler loading. This was due to increasing composition of potash feldspar in the EVA/NR/PF composites. However from Table 3, at similar filler loading, the EVA/NR/PF$_{Silane}$ composites exhibit lower percentage of crystallinity value than EVA/NR/PF composites. This was due to enhanced interfacial adhesion between EVA/NR phases with the potash feldspar which improved the chain flexibility of the EVA/NR/PF$_{Silane}$ composites.

Figure 8 shows the TG thermograms of EVA/NR/PF$_{Silane}$ composites at different PF loading while Table 4 shows the temperature at 50% weight loss ($T_{-50\%\ wt}$), residual mass and final decomposition temperature (FDT) of EVA/NR/PF composites with and without silane

Penerbit Akademia Baru
Journal of Advanced Research in Materials Science
ISSN (online): 2289-7992 | Vol. 11, No.1. Pages 8-19, 2015

treatment. The $T_{-50\%\ wt}$ and residual mass for both composites increased but FDT decreased as the filler loading increased. EVA/NR/PF_{Silane} composites have higher $T_{-50\%\ wt}$ but lower FDT and residual mass compared to EVA/NR/PF composites. EVA/NR/PF_{Silane} composites exhibited higher thermal stability in comparison with EVA/NR/PF composites. This could be attributed to the ability of the feldspar to absorb the heat faster than the polymer matrix and hence protecting the polymer matrix from the heat.

Table 3: Melting temperature (T_m) and degree of crystallinity of EVA/NR/PF and EVA/NR/PF_{Silane} composites at different PF loading

Composites Code	T_m (°C)	Percentage of Crystallinity (%)
EVA/NR	110.96	93.41
EVA/NR/5PF	85.83	44.96
EVA/NR/15PF	85.90	45.13
EVA/NR/25PF	85.97	45.84
EVA/NR/5PF_{Silane}	85.87	34.54
EVA/NR/15PF_{Silane}	85.93	34.41
EVA/NR/25PF_{Silane}	86.17	31.53

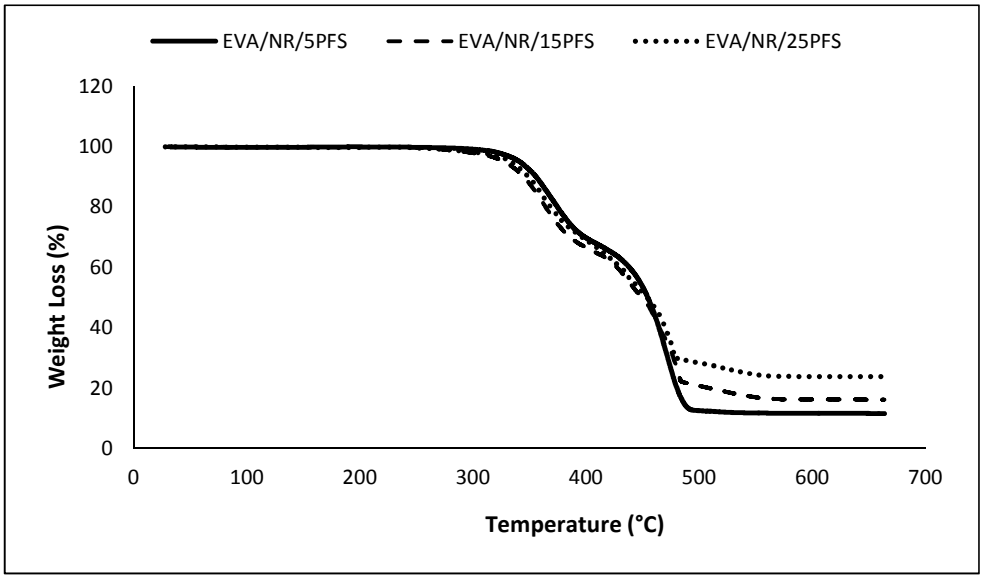

Figure 8: TG thermograms of EVA/NR/5PF_{Silane}, EVA/NR/15PF_{Silane} and EVA/NR/25PF_{Silane} composites

Linkages formed by one end of the silane functional group with the PF and the other end react with the matrix had improved the thermal stability in which higher heat are required to break the strong bond. Mousa [15] observed that as the feldspar loading increased, the percentage of weight retained has increased. He claimed that the thermal stability of the R-PET/SMRL had been improved with the feldspar loading. This may related to the ability of feldspar to absorb heat. Liu et al. [16] claimed that the strong interaction between matrix and filler are the reason for the increasing degree of thermal stability for the silane coupling agent γ-methacryloxypropyl trimethoxy modified tremolite blend with PA1010 (polydecamethylene

esbacamide). Maziad et al. [17] claimed that rice husk (RH) treated by 3-APE silane showed superior thermal stability and crosslink density compared to untreated NR/LDPE blend sample with RH.

Table 4: Temperature at 50 % weight loss ($T_{-50\%\ wt}$), residualmass and final decomposition temperature (FDT) of EVA/NR/PF and EVA/NR/PF_{Silane} different PF loading

Composites Code	$T_{-50\%\ wt}$	FDT	Residual Mass (%)
EVA/NR	430.87	704.93	2.04
EVA/NR/5PF	416.89	704.91	9.583
EVA/NR/15PF	432.75	704.85	16.293
EVA/NR/25PF	437.62	704.72	24.498
EVA/NR/5PF_{Silane}	454.15	664.10	11.616
EVA/NR/15PF_{Silane}	454.22	663.87	16.275
EVA/NR/25PF_{Silane}	454.68	660.01	23.894

CONCLUSION

The function of filler treated with silane coupling agent is to improve the compatibility. For EVA/NR/PF_{Silane} composites, the tensile strength and M100 were increased while the elongation at break and mass swell were decreased. EVA/NR/PF_{Silane} composites exhibited lower degree of crystallinity but higher thermal stability in comparison to EVA/NR/PF composites. The interfacial adhesion between filler and polymer matrix was also improved with the treatment of the filler with silane coupling agent.

REFERENCES

[1] W. Pechurai, C. Nakason, K. Sahakaro, Thermoplastic natural rubber based on oil extended NR and HDPE blends: Blend compatibilizer, phase inversion composition and mechanical properties, Polymer Testing 27 (2008) 621-631.

[2] Y.W. Chang, J.K. Mishra, S.K. Kim, D.K. Kim, Effect of supramolecular hydrogen bonded network on the properties of maleated ethylene propylene diene rubber/maleated high density polyethylene blend based thermoplastic elastomer, Materials Letters 60 (25-26) (2006) 3118-3121.

[3] U. Eisele, Deformation Behavior of Thermoplastic Elastomers, Springer Berlin Heidelberg: German, 1990, pp. 147-155.

[4] V. Chalivendra, B. Song, D. Casem, Dynamic Behavior of Materials, in: V. Kushvaha, A. Branch and H. Tippur, Proceedings of the 2012 Annual Conference on Experimental and Applied Mechanics, Springer, California, 2012, pp. 169-176

[5] A.K. Kulshreshtha, C. Vasile, Handbook of Polymer Blends and Composites, Rapra Technology Limited, United Kingdom, 2002, pp. 39-96.

[6] J.C.J. Bart, Plastics Additives: Advanced Industrial Analysis, IOS Press, Netherlands, 2006, pp. 779-783.

[7] A. Boudenne, L. Ibos, Y. Candau, S. Thomas, Handbook of Multiphase Polymer Systems, Wiley, United Kingdom, 2011, pp. 1-12.

[8] Y. Xie, C.A.S. Hill, Z. Xiao, H. Militz, C. Mai, Silane coupling agents used for natural fiber/polymer composites: A review, Composites Part A: Applied Science and Manufacturing 41 (2010) 806-819.

[9] C. Cercle and B.D. Favis, Generalizing interfacial modification in polymer blends, Polymer 53 (2012) 4338-4343.

[10] K.A. Moly, H.J. Radusch, R. Androsh, S.S. Bhagawan, S. Thomas, Nonisothermal crystallisation, melting behavior and wide angle X-ray scattering investigations on linear low density polyethylene (LLDPE)/ethylene vinyl acetate (EVA) blends: effects of compatibilisation and dynamic crosslinking, European Polymer Journal 41 (2005) 1410-1419.

[11] N.A.N. Alkadasi, D.G. Hundiwale, U.R. Kapadi, Studies on the effect of silane coupling agent (2.0 per cent) on the mechanical properties of flyash filled polybutadiene rubber Journal of Scientific & Industrial Research 63 (2004) 603-609.

[12] S. Ganguly, P. Bhattacharya, A.N. Banerjee, Effect of surface modification of carbon black by 1,2 dihydroxy benzene and 1,2,3 trihydroxy benzene on a natural rubber-carbon black composite, Indian Journal of Chemical Technology 12 (2005) 695-700.

[13] S.J. Park, K.S. Cho, Filler- elastomer interactions: influence of silane coupling agent on crosslink density and thermal stability of silica/rubber composites, Journal of Colloid and Interface Science 267 (2003) 86-91.

[14] W. Bigui, C. Qing, C. Bao, L. Dai, G. Zhang, F. Wu, Surface modification of filter medium particles with silane coupling agent KH550, Colloids and Surfaces A: Physicochemical and Engineering Aspects 434 (2013) 276-280.

[15] A. Mousa, On the potential of feldspar sand for recycled PET/SMRL composites, Journal of Elastomers and Plastics 40 (2008) 179-190.

[16] X.L. Liu, Y. Hana, G. Gao, Z.Y. Li, F.Q. Liu, Effect of silane coupling agent on the mechanical, thermal properties and morphology of tremolite/pa1010 composites, Chinese Journal of Polymer Science 26 (2008) 255-262.

[17] N.A. Maziad, D.E. El-Nashar, E.M. Sadek, The effects of a silane coupling agent on properties of rice husk-filled maleic acid anhydride compatibilized natural rubber/low-density polyethylene blend, Journal of Materials Science 44 (2009) 2665-2673.